

Electronic Supplementary Information †

Direct Access to Aggregation-Free and Small Intermetallic Nanoparticles in Ordered, Large-Pore Mesoporous Carbon for Electrocatalyst

*Yeongdong Mun, Jongmin Shim, Kyeounghak Kim, Jeong Woo Han, Soo-Kil Kim, Youngjin Ye, Jongkook Hwang, Seonggyu Lee, JongHyun Jang, Yong-Tae Kim, Jinwoo Lee**

Experimental Details

Synthesis of M-x-OMCAs and M-x-OMCSs.

Aluminosilicate sol was prepared by sol-gel process of a mixture of two metal alkoxide, (3-glycidyloxypropyl) trimethoxysilane, GLYMO, with aluminum *sec*-butoxide, Al(O^{*s*}Bu)₃.^{S1} The molar ratio of silicon and aluminum was fixed as 9:1. The block co-polymer PS-*b*-PEO (PDI: 1.08) with M_n = 33,000 g mol⁻¹ and 15.2 wt% PEO was synthesized by atom transfer radical polymerization (ATRP).^{S2, 3} A typical procedure for the synthesis of Pt-x-OMCA was as follows: 0.2 g of PS-*b*-PEO was dissolved in tetrahydrofuran (THF) (5 g). After the aluminosilicate sol (0.457 g) and resol solution^{S4} (carbon precursor, 1.71 g, 20 w/v % in THF) were added to the polymer-metal precursor solution, a targeted amount of Dimethyl-(1,5-cyclooctadiene)-platinum(II) (Strem Chemicals) was also added. The mixture was further stirred for 1 h at room temperature and poured into a petri-dish. The as-made film was collected by evaporation of solvents on a hot plate at 50 °C and further annealed at 100 °C. Subsequent heat treatment was carried out in a furnace at 450 °C for 3 h and subsequently at 700 °C for 2 h under 4% H₂/Ar. The heating rate was 1 °C/min. For the synthesis of Pt-5-OMCS, where OMCS refers to ordered mesoporous carbon/silica, tetraethylorthosilicate (TEOS, 0.397 g, Sigma-Aldrich) was used as a silica precursor.

The same procedures were carried out for the preparation of sample PtPb-20-OMCA and Pt₃CO-20-OMCA. For the intermetallic PtPb particles, dimethyl-(1,5-cyclooctadiene)-platinum(II) and triphenyl(phenylethynyl)-lead (98%, Sigma-Aldrich) were used as a Pt and Pb precursor, respectively. For the intermetallic Pt₃Co, dimethyl-(1,5-cyclooctadiene)-platinum(II) and cobalt (II) phthalocyanine (Sigma-Aldrich) were used. The aluminosilicate or

silica framework in Pt₃Co containing catalyst was removed with 10 wt% HF solution for 2 h before electrochemical characterizations.

Material Characterization

²⁷Al magic-angle spinning (MAS) spectrum was recorded by Bruker Avance II (500 MHz) spectrometer with a frequency of 130.32 MHz. Short pulse of 1.3 μs duration was used (pulse angle of about 22°), the repetition time was 1.5s, and the spinning speed was 12 kHz. Powder X-ray diffraction (XRD) data were collected using a Max-2500 diffractometer (RIKAGU, Cu Kα, 1.5418 Å). The morphology of samples was observed using a transmission electron microscope (TEM, Hitachi H-7600) operated at 100 kV and a scanning electron microscope (SEM, Hitachi S-4800). For TEM, the samples were microtomed with 100 nm section thickness. High-resolution TEM (HR-TEM) images were obtained with a JEOL JEM-2200FS instrument operated at 200 kV. Tristar II 3020 system (Micromeritics Inc.) at 77 K was used to measure nitrogen physisorption. The samples degassed over 12 hours at 150 °C before measurement. Pore size distribution plots were obtained by BJH method with N₂ adsorption branches.^{S5} Small-angle X-ray scattering (SAXS) experiments were carried out on the 4C SAXS station at the Pohang Accelerator Laboratory (PAL, Korea). Inductively coupled plasma (ICP) spectroscopy and thermogravimetric analysis (TGA) were used to measure the actual loading amount of Pt, PtPb, and Pt₃Co nanoparticles in the composites. X-ray photoelectron spectroscopy (XPS) data were obtained with a VG Scientific Escalab 250 using an Al Kα source.

Computational Methods

We performed plane-wave DFT calculations using the Vienna ab initio Simulation Package (VASP).^{S6, 7} The exchange-correlation functional was treated at the level of GGA using its Perdew–Burke–Ernzerhof variant (GGA-PBE).^{S8} A plane wave expansion with a cutoff of 400 eV was used with a $2 \times 2 \times 1$ Monkhorst-Pack^{S9} k -point sampling of the Brillouin zone, which was sufficient to give well converged results. In all calculations, the projected augmented wave (PAW) potentials^{S10} with the valence states 6s, 5d for Pt, 3s, 3p for Al, 2s, 2p for O, and 3s, 3p for Si have been employed, respectively. Total energy calculations used the residual minimization method for electronic relaxation and geometries were relaxed using a conjugate gradient algorithm until the forces on all unconstrained atoms were less than 0.03 eV/Å.

To represent the surface of the amorphous SiO₂, β -cristobalite (001) was used, which has been often used for this purpose due to their similar physical properties to amorphous SiO₂.^{S11-14} Detailed explanation about the model can be found in the previous report.^{S15} The DFT-optimized lattice constant is found to be 5.02 Å (a,b) and 7.38 Å (c), which is in agreement with the experimentally reported values.^{S16} The surface was constructed by cleaving along the (001) plane. A vacuum thickness of ~ 20 Å was used to decouple the periodic images of the slab of silica surfaces. Dangling oxygens on the surface were fully hydroxylated by adding equal number of hydrogens. The surface consisted of 8 layers (4 Si layers and 4 O layers). The top four layers were allowed to relax while the remaining four bottom layers were fixed. To model aluminosilicate support, one Si atom was replaced with one Al atom on the surface in the unit cell. The energy of the isolated Pt atom was calculated in a large cubic cell of 10 Å in length. The binding energy of Pt atom onto the SiO₂ substrate was calculated by

$$E_{\text{ads}} = E_{\text{Pt/SiO}_2} - (E_{\text{SiO}_2} + E_{\text{Pt}})$$

, where E_{Pt/SiO_2} , E_{SiO_2} and E_{Pt} refer to the total energy of the system containing the adsorbed Pt atom, the optimized bare SiO₂ surface, and free atom in vacuum, respectively. To provide insight into the origins in surface binding, charge density differences were calculated for the adsorbate substrate system according to

$$\Delta\rho = \rho_{Pt/SiO_2} - (\rho_{SiO_2} + \rho_{Pt})$$

, where ρ_{Pt/SiO_2} is the charge density of the total system, ρ_{SiO_2} is the charge density of the silica surface fixed at the adsorbed geometry, and ρ_{Pt} is the electron density of a isolated Pt atom. Bader charge analysis was conducted using a grid-based algorithm.^{S17} The charge on an atom was defined as the difference between the valence charge and the Bader charge.

Electrochemical measurements – Formic acid oxidation reaction

The catalytic ink for preparation of working electrodes consisted of PtPb-20-OMCA (or PtPb-9-OMCS) catalysts dispersed in a mixed solution of 2-propanol, and a 5% w/w alcoholic solution of Nafion® (Aldrich). The ratio of catalyst to Nafion solution was 1 mg to 10 µl. The resulting mixture was sonicated in a bath-type ultrasonicator for 60 min before being dropped onto the surface of a glassy carbon electrode (GCE) with 6 mm diameter, and then dried under ambient atmosphere at room temperature for 12 hours. Commercial Pt/C (10wt%) and Pd/C (10 wt%) electrode were prepared by the same method. The catalysts-coated GCEs were rotated at 2000 rpm to minimize the possible blockage of catalytic active sites on the surface by bubbles formed during FA oxidation. Prior to all of the electrochemical measurements, the catalyst containing electrode was pre-treated in a 0.1 M H₂SO₄ aqueous solution for 30 min between -0.2 and +0.2 V ten times at 10 mV/s to clean the catalyst surface. Cyclic voltammetry

(CV) measurements were performed for FOR at a scan rate of 10 mV/s in an aqueous solution of 0.1 M H₂SO₄ containing 0.5 M formic acid in the range of -0.2 to +0.2 V (vs. Ag/AgCl).

CO stripping experiment was conducted in 0.1 M H₂SO₄ solution. After obtaining CV curves in nitrogen purged solution between -0.2 and 0.65 V with a scan rate of 50 mV/s, CO gas (99.9 %) was purged into the solution containing the electrode for 30 min while maintaining the electrode potential at -0.12 V followed by bubbling nitrogen gas for 30 min. The CO stripping curves were obtained with the same voltage range and scan rate. Chronoamperometry for comparing durability was conducted at 0.5 M formic acid and 0.1 M H₂SO₄ solution at 0.3 V with static condition, while the nitrogen gas was purged into the solution.

Electrochemical measurements – Oxygen reduction reaction

For measurement of ORR activity of the catalysts, the catalytic ink and the metal loading was adjusted to 15 μg/cm². The slurry was made by the same manner with making the slurry for FOR. CV measurement was performed on the electrode in N₂ purged 0.1 M HClO₄ solution in the range of 0.05 to 1.0 V (vs. RHE) with a scan rate of 50 mV/s. Electrochemical surface area of the catalyst was calculated by integrating the hydrogen adsorption/desorption region between 0.05 and 0.40 V and by using a conversion factor of 200 μC/cm² (equation S3).^{S18} The ORR polarization curves were obtained by linear sweep voltammetry from 0.05 to 1.0 V at a scan rate of 20 mV/s and rotation rate of 1600 rpm. Pt/C (40wt%, Johnson-Matthey) was tested in the same condition for comparison. For evaluating the durability of the catalysts, 3000 and 10000 times potential cycling was performed between 0.6 and 1.1 V (vs. RHE in N₂-purged 0.1M HClO₄ solution).

Table S1. BET surface areas

Samples	BET surface area (m ² /g)
Pt-5-OMCA	340
Pt-20-OMCA	312
Pt-5-OMCS	311
Pt-20-OMCS	252

Table S2. The composition of M-x-OMCA.

Sample	Metal ^[a] (wt%)	Carbon ^[b]	Aluminosilicate
OMCA	0	60	40
Pt-5-OMCA	Pt: 5	57	38
Pt-20-OMCA	Pt: 20.4	47.8	31.8
PtPb-20-OMCA	Pt: 9.81 Pb: 10.39 Molar Pt/Pb ratio: 1.004	47.9	31.9
Pt ₃ Co-33-OMC(A)	Pt: 29.76 Co: 2.94 Molar Pt/Co ratio: 3.06	67.3	0

[a] Metal contents were determined by ICP analysis.

[b] The relative weight fraction of carbon/aluminosilicate (or carbon/silica) was targeted to 6/4.

Table S3: BET surface areas

Samples	BET surface area (m²/g)
PtPb-20-OMCA	339
Pt ₃ Co-33-OMC(A)	1048

Table S4. Comparison of mass activities: Catalysts of PtPb on carbon support tested in 0.5 M formic acid and 0.1M H₂SO₄ solution with a scan rate of 10 mV/s and 2000 rpm for FOR from the previous reports and this work.

Reference paper	Synthesis method	Electrolyte	Scan rate (rotating speed)	Mass activity (A/mg _{metal}) at 0.2 V (converted to vs. Ag/AgCl)
[1] ^{S19}	Sodium naphthalide reduction	0.5 M HCOOH, 0.1 M H ₂ SO ₄	10 mV/s (2000 rpm)	0.045
[2] ^{S20}	NaBH ₄ reduction	0.5 M HCOOH, 0.1 M H ₂ SO ₄	10 mV/s (2000 rpm)	0.042
[3] ^{S21}	NaBH ₄ reduction	0.5 M HCOOH, 0.1 M H ₂ SO ₄	10 mV/s (2000 rpm)	0.13
[4] ^{S22}	Block-copolymer assisted one-pot synthesis	0.5 M HCOOH, 0.1 M H ₂ SO ₄	10 mV/s (2000 rpm)	1.14
This paper	Block-copolymer assisted one-pot synthesis	0.5 M HCOOH, 0.1 M H ₂ SO ₄	10 mV/s (2000 rpm)	2.07

Table S5. Comparison of durability of catalysts which were reported recently in FOR condition.

Reference paper	Material	Voltage for stability test	Current retention after 1800 seconds ^a (%)
This work	PtPb-20-OMCA		57
This work	Pd/C	0.3 V vs. Ag/AgCl	12
This work	Pt/C		55
[1] ^{S23}	PdAg/Ti _{0.5} Cr _{0.5} N	0.6 V vs. RHE	17
[2] ^{S24}	PdNi-nanowire networks on RGO	0.25 V vs. SCE	7
[3] ^{S25}	Nanobranched PdSn intermetallic	0.15 V vs. SCE	26
[4] ^{S26}	PtAu/Graphene	0.3 V vs. RHE	38
[5] ^{S27}	Pd-Au/PDDA-Graphene	0.3V vs. Ag/AgCl	86

^a Standard of 1800 seconds was selected to compare the current retention of the reported catalysts at same time.

Table S6. Mass activities (0.9 V vs. RHE) for ORR before and after 3000 and 10000 cycles of durability test (0.6 ~ 1.1 V vs. RHE)

Samples	Mass activity (mA/mg _{cat})		
	initial	After 3000 cycles	After 10000 cycles
Pt/C 40wt%	105	50	35
Pt ₃ Co-31-OMC(S)	215	181	140
Pt ₃ Co-33-OMC(A)	342	249	202

Table S7. ECSA obtained from CO stripping (ECSA_{CO}) and H_{upd} ($\text{ECSA}_{\text{Hupd}}$) for Pt/C 40wt%, $\text{Pt}_3\text{Co-31-OMC(S)}$, and $\text{Pt}_3\text{Co-33-OMC(A)}$.

Samples	ECSA_{CO}	$\text{ECSA}_{\text{Hupd}}$	$\text{ECSA}_{\text{CO}}/\text{ECSA}_{\text{Hupd}}$
Pt/C 40wt%	74	66	1.11
$\text{Pt}_3\text{Co-31-OMC(S)}$	48	32	1.50
$\text{Pt}_3\text{Co-33-OMC(A)}$	93	83	1.12

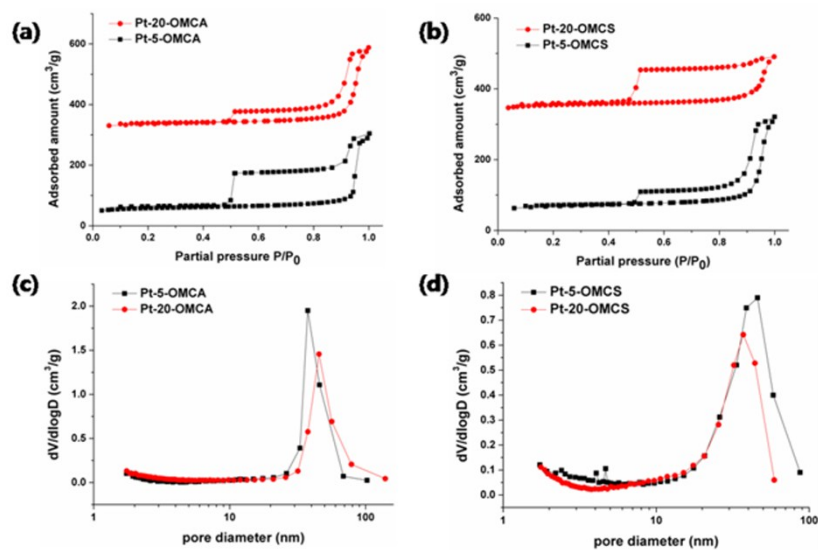


Fig. S1 N₂ physisorption data for Pt on OMCSs and OMCA: Linear isotherm adsorption/desorption plots of (a) Pt-5-OMCA, Pt-20-OMCA, (b) Pt-5-OMCS, and Pt-20-OMCS. Pore size distributions of (c) Pt-5-OMCA, Pt-20-OMCA, (d) Pt-5-OMCS, and Pt-20-OMCS.

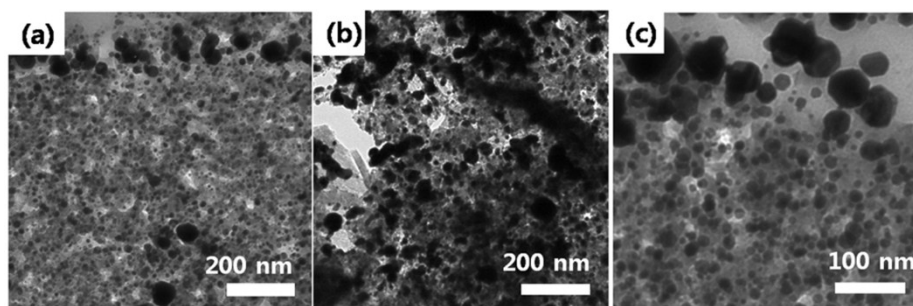


Fig. S2 When large amount of metal (> 20 wt%) was loaded on OMCS support, the mesoporous structure was destroyed in some part, because the metal particles were significantly sintered and grew larger than mesopore size of OMCS. The destruction of mesoporous structure was observed in not only (a) Pt-20-OMCS, also in the intermetallic based systems of (b) PtPb-20-OMCS and (c) Pt₃Co-31-OMC(S).

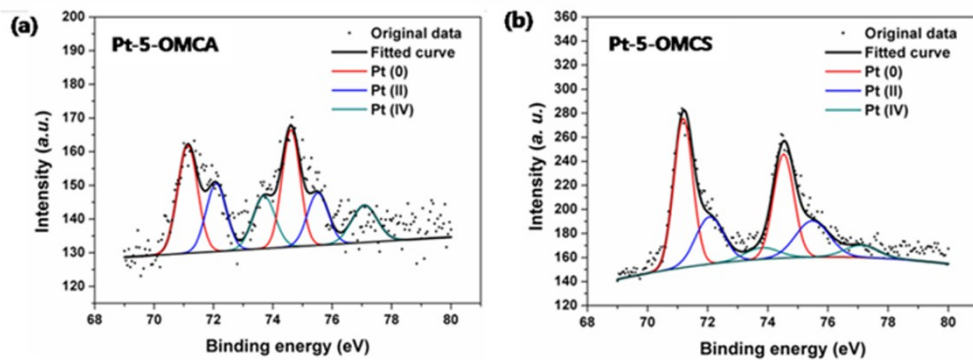


Fig. S3 Pt_{4f} XPS spectra and the deconvoluted peaks: (a) Pt-5-OMCS and (b) Pt-5-OMCA. The spectra were deconvoluted to peaks near 72.3 eV and 73.8 eV corresponding to Pt (II) and Pt (IV), respectively, in addition to zero valent state (Pt (0), centered 71.1 eV).^{S28}

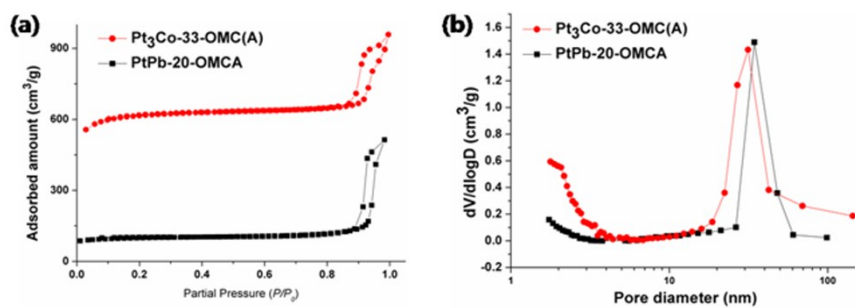


Fig. S4 N₂ physisorption data for sample of Pt-intermetallic on OMCA supports: (a) Linear isotherm adsorption/desorption plots and (b) pore size distributions of PtPb-20-OMCA and Pt₃Co-33-OMC(A).

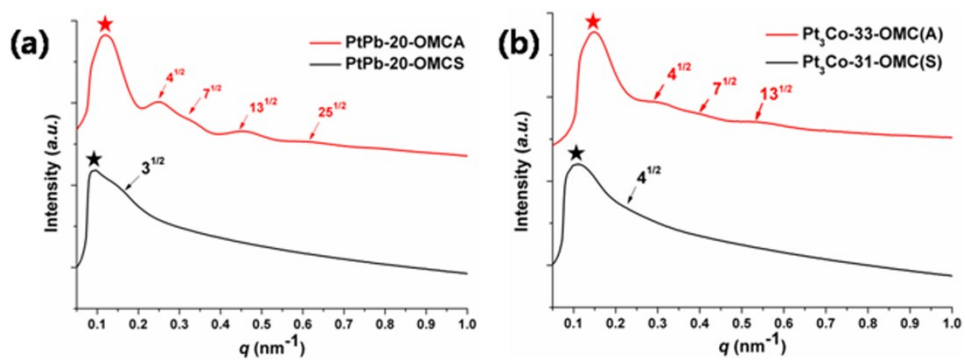


Fig. S5 SAXS patterns for sample of Pt-intermetallic nanoparticles on OMCA and OMCS: (a) PtPb-20-OMCA, PtPb-20-OMCS, (b) Pt₃Co-33-OMC(A), and Pt₃Co-31-OMC(S). The asterisks indicate the first order peaks.

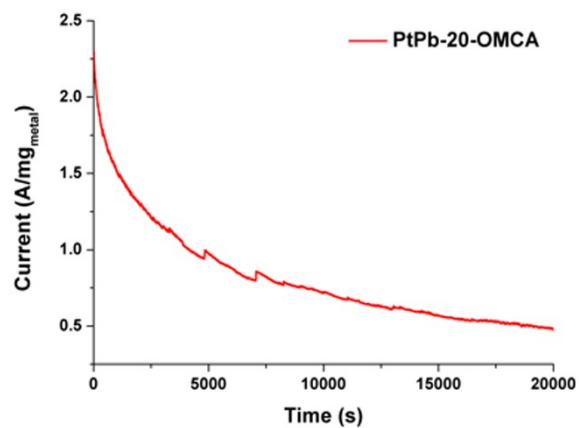


Fig. S6 Chronoamperometry result of PtPb-20-OMCA for FOR: 20000 seconds at 0.3 V (vs. Ag/AgCl) in 0.5 M formic acid and 0.1 M H₂SO₄ solution.

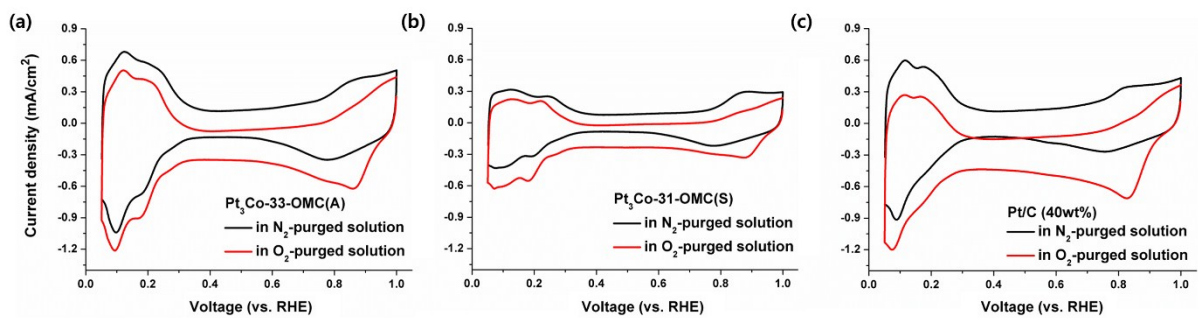


Fig. S7 Cyclic voltammety curves in N_2 and O_2 purged 0.1M $HClO_4$ solution: (a) Pt_3Co -33-OMC(A), (b) Pt_3Co -31-OMC(S), and (c) Pt/C 40wt%.

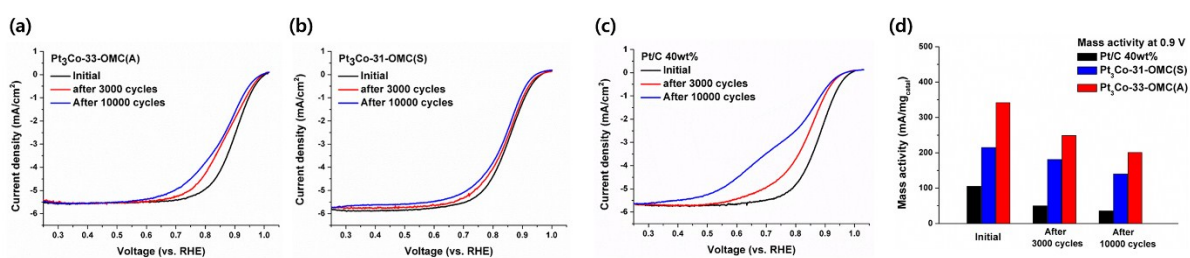


Fig. S8 ORR polarization curves before and after 3000 and 10000 potential cycles between 0.6 and 1.1 V (vs. RHE in Ar-purged 0.1 M HClO₄): (a) Pt₃Co-33-OMC(A), (b) Pt₃Co-31-OMC(S), (c) Pt/C 40wt%. (d) Comparison of the mass activities (at 0.9 V vs. RHE) of the tested samples before and after 3000 and 10000 potential cycles.

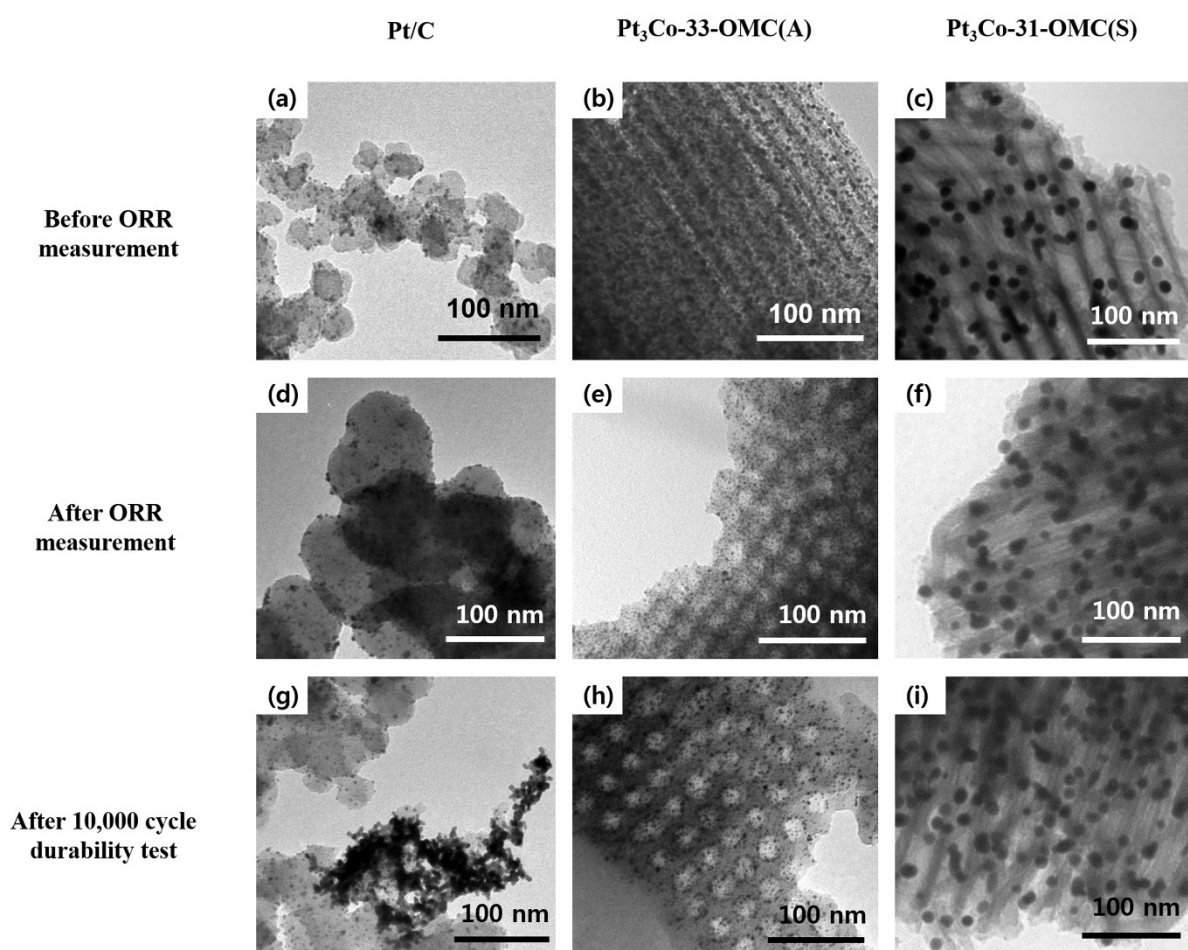


Fig. S9 TEM images of as-prepared catalysts ((a) Pt/C; (b) Pt₃Co-33-OMC(A); (c) Pt₃Co-31-OMC(S)), catalysts obtained after ORR measurements ((d) Pt/C; (e) Pt₃Co-33-OMC(A); (f) Pt₃Co-31-OMC(S)), and catalysts obtained after durability tests of 10000 potential cycles ((g) Pt/C; (h) Pt₃Co-33-OMC(A); (i) Pt₃Co-31-OMC(S)).

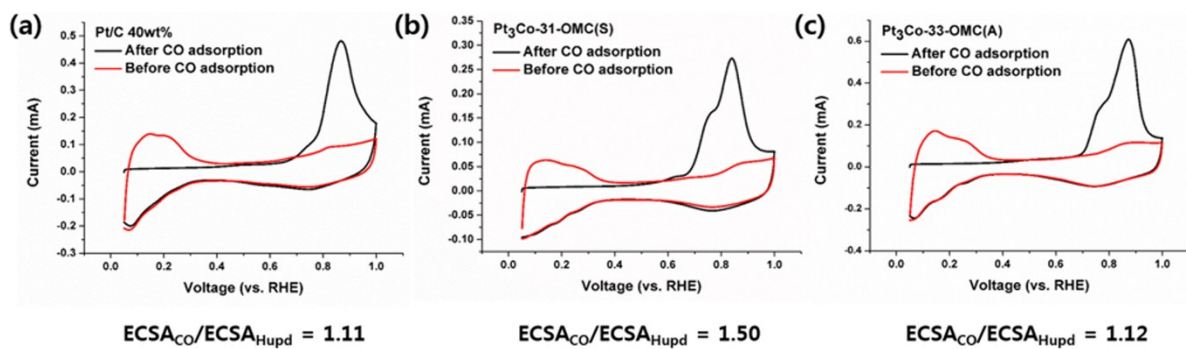


Fig. S10 ECSA measurement by CO stripping and H_{upd} : (a) Pt/C 40 wt%, (b) Pt₃Co-31-OMC(S), and (c) Pt₃Co-33-OMC(A).

$$\frac{1}{j_{measured}} = \frac{1}{j_k} + \frac{1}{j_d}$$

Equation S1. Koutecky-Levich equation that describes the relationship between the measured current density ($j_{measured}$ (mA/cm²)), kinetic current density (j_k (mA/cm²)), and diffusion limiting current density (j_d (mA/cm²)).

$$j_{mass} = \frac{j_k}{m_{catal}}$$

Equation S2. Relation between mass activity (j_{mass} (mA/mg)) and kinetic activity (j_k (mA/cm²))

$$ECSA = \frac{Q_{ads}}{m_{catal} \times C_{char}}$$

Equation S3. Equation for obtaining Electrochemical surface area ($ECSA$ (m²/g)), where Q_{ads} (C) is cumulative charge, m_{catal} (mg) is mass of catalyst, and C_{char} (C/m²) is charge per one molecule adsorption.

$$j_{specific} = \frac{j_m}{ECSA}$$

Equation S4. Relation between mass activity (j_{mass} (mA/mg)) and specific activity ($j_{specific}$ (mA/cm_{catal}²))

References in Supplementary Information

- S1. P. F. W. Simon, R. Ulrich, H. W. Spiess and U. Wiesner, *Chem. Mater.*, 2001, **13**, 3464-3486.
- S2. J.-S. Wang and K. Matyjaszewski, *J. Am. Chem. Soc.*, 1995, **117**, 5614-5615.
- S3. J. Hwang, J. Kim, E. Ramasamy, W. Choi and J. Lee, *Microporous Mesoporous Mater.*, 2011, **143**, 149-156.
- S4. R. Liu, Y. Shi, Y. Wan, Y. Meng, F. Zhang, D. Gu, Z. Chen, B. Tu and D. Zhao, *J. Am. Chem. Soc.*, 2006, **128**, 11652-11662.
- S5. E. P. Barrett, L. G. Joyner and P. P. Halenda, *J. Am. Chem. Soc.*, 1951, **73**, 373-380.
- S6. G. Kresse and J. Furthmüller, *Phys. Rev. B*, 1996, **54**, 11169-11186.
- S7. J. A. S. D.S. Sholl, *Density functional theory: a practical introduction*, John Wiley & Sons, Inc.Hoboken, NJ, 2009.
- S8. J. P. Perdew, K. Burke and M. Ernzerhof, *Phys. Rev. Lett.*, 1996, **77**, 3865-3868.
- S9. H. J. Monkhorst and J. D. Pack, *Phys. Rev. B*, 1976, **13**, 5188-5192.
- S10. P. E. Blöchl, *Phys. Rev. B*, 1994, **50**, 17953-17979.
- S11. D. W. Sindorf and G. E. Maciel, *J. Am. Chem. Soc.*, 1983, **105**, 1487-1493.
- S12. I. S. Chuang and G. E. Maciel, *J. Phys. Chem. B*, 1997, **101**, 3052-3064.
- S13. L. T. Zhuravlev, *Langmuir*, 1987, **3**, 316-318.
- S14. J. B. Peri and A. L. Hensley, *J. Phys. Chem.*, 1968, **72**, 2926-2933.
- S15. J. Handzlik and J. Ogonowski, *J. Phys. Chem. C*, 2012, **116**, 5571-5584.
- S16. A. F. Wright and A. J. Leadbetter, *Philos. Mag.*, 1975, **31**, 1391-1401.
- S17. R. F. W. Bader, *Atoms in molecules: A quantum theory*, ClarendonPress, Oxford, UK, 1990.
- S18. F. J. Vidal-Iglesias, R. M. Arán-Ais, J. Solla-Gullón, E. Herrero and J. M. Feliu, *ACS*

- Catal.*, 2012, **2**, 901-910.
- S19. L. R. Alden, D. K. Han, F. Matsumoto, H. D. Abruña and F. J. DiSalvo, *Chem. Mater.*, 2006, **18**, 5591-5596.
- S20. L. R. Alden, C. Roychowdhury, F. Matsumoto, D. K. Han, V. B. Zeldovich, H. D. Abruña and F. J. DiSalvo, *Langmuir*, 2006, **22**, 10465-10471.
- S21. F. Matsumoto, C. Roychowdhury, F. J. DiSalvo and H. D. Abruña, *J. Electrochem. Soc.*, 2008, **155**, B148-B154.
- S22. J. Shim, J. Lee, Y. Ye, J. Hwang, S.-K. Kim, T.-H. Lim, U. Wiesner and J. Lee, *ACS Nano*, 2012, **6**, 6870-6881.
- S23. Z. Cui, M. Yang and F. J. DiSalvo, *ACS Nano*, 2014, **8**, 6106-6113.
- S24. D. Bin, B. Yang, F. Ren, K. Zhang, P. Yang and Y. Du, *J. Mater. Chem. A*, 2015, **3**, 14001-14006.
- S25. D. Sun, L. Si, G. Fu, C. Liu, D. Sun, Y. Chen, Y. Tang and T. Lu, *J. Power Sources*, 2015, **280**, 141-146.
- S26. S. Zhang, Y. Shao, H. Liao, J. Liu, I. A. Aksay, G. Yin and Y. Lin, *Chem. Mater.*, 2011, **23**, 1079-1081.
- S27. T. Maiyalagan, X. Wang and A. Manthiram, *RSC Adv.*, 2014, **4**, 4028-4033.
- S28. L. K. Ono, B. Yuan, H. Heinrich and B. R. Cuenya, *J. Phys. Chem. C*, 2010, **114**, 22119-22133.